

**DEVELOPMENT OF AN IMPROVED ALGORITHM OF MPPT  
TECHNIQUE FOR PHOTOVOLTAIC POWER GENERATION**

**MUHAMMAD HAFEEZ BIN MOHAMED HARIRI**

**UNIVERSITI SAINS MALAYSIA**

**2013**

**DEVELOPMENT OF AN IMPROVED ALGORITHM OF MPPT  
TECHNIQUE FOR PHOTOVOLTAIC POWER GENERATION**

**by**

**MUHAMMAD HAFEEZ BIN MOHAMED HARIRI**

**Thesis submitted in fulfillment of the requirements**

**for the Degree of**

**Master of Science**

**June 2013**

## ACKNOWLEDGEMENTS

First and foremost, I would like to thank Allah for His mercy and love on me during all my life. I dedicate this research work to my late father (Mohamed Hariri Abdul Rahman) and to all my family members. Furthermore, I would like to express my sincere gratitude and thanks towards my main supervisor Dr. Ir. Syafrudin Masri and co-supervisor Dr. Norizah Mohamad for their guidance, motivation and continuous support throughout the completion of this research and preparing this thesis. Their attitude, enthusiasm and passion towards knowledge, has boosted my desire to work hard and willing to sacrifice to achieve more success in future. Besides, their invaluable support and insightful suggestions not to mention all the shared knowledge and extra time poured contributed towards finishing this research.

Special acknowledgement goes to the Ministry of Higher Education Malaysia (MyBrain15) and School of Electrical and Electronics Engineering, Universiti Sains Malaysia (USM) for the awarded financial support to do this research. Moreover, I also would like to extend my thankful towards the technical staffs at the School of Electrical and Electronics Engineering for their assistance and cooperation throughout my research progress. My thanks are also reserved for other academic and administrative staffs, which have been helping me directly or indirectly towards finishing this thesis.

Finally, my deepest gratitude and special thanks goes to my friends for their understandings, moral supports and encouragement during the past months. Without helps of the above mentioned people, I would face difficulties while doing this research. May Allah bless all of us with His mercy.

Muhammad Hafeez Bin Mohamed Hariri

## TABLE OF CONTENTS

	Page
<b>ACKNOWLEDGEMENTS</b>	ii
<b>TABLE OF CONTENTS</b>	iii
<b>LIST OF TABLES</b>	vii
<b>LIST OF FIGURES</b>	viii
<b>LIST OF PLATES</b>	xi
<b>LIST OF SYMBOLS</b>	xii
<b>LIST OF ABBREVIATION</b>	xv
<b>ABSTRAK</b>	xvi
<b>ABSTRACT</b>	xvii
<b>CHAPTER 1 - INTRODUCTION</b>	
1.1 Research Motivations	1
1.2 Problem Statements	4
1.3 Research Objectives	4
1.4 Research Approach	5
1.5 Thesis Outline	6
1.6 Research Contributions	8
<b>CHAPTER 2 - LITERATURE REVIEW</b>	
2.1 Introduction	9
2.2 Renewable Energy	9
2.3 Solar Energy	10
2.4 Principle Operation of Photovoltaic (PV)	11
2.5 DC-DC Buck Converter	14

2.5.1	Principle of Operation	15
2.6	Principle Operation of Maximum Power Point Tracking, MPPT	22
2.7	Photovoltaic Control Strategy	23
2.7.1	Hill Climbing (HC)	24
2.7.2	Perturbation and Observation (P&O)	25
2.7.3	Modify Perturbation and Observation (MP&O)	28
2.7.4	Incremental Conductance (INC)	30
2.7.5	Fractional Open Circuit Voltage	31
2.7.6	Fractional Short Circuit Current	32
2.7.7	Fuzzy Logic, Neural Network and Other Algorithms	32
2.6	Concluding Remark	34

### **CHAPTER 3 - METHODOLOGY**

3.1	Introduction	35
3.2	Potential of Solar Energy at Nibong Tebal Areas	37
3.3	Design of Digital MPPT Controller	39
3.4	Design of a Synchronous DC-DC Buck Converter	41
3.4.1	Operation of Synchronous DC-DC Buck Converter	43
3.5	An Improved Perturbation & Observation MPPT Algorithm	45
3.6	Simulation	46
3.6.1	PV Model	47
3.6.2	Circuit Oriented Model of PV Module	51
3.6.3	Design of DC-DC Buck converter in Matlab-Simulink	52
3.6.4	Complete System of PV with MPPT Control Circuit in Simulink	53
3.7	Hardware Implementation of PV System with MPPT Technique	54
3.7.1	Miscellaneous Consideration of the Prototype Design	55
3.7.2	Health Davis Instruments	56

3.7.3	Power Switch	57
3.7.4	Inductor	59
3.7.5	Freewheeling Diode	59
3.7.6	MOSFET Driver	60
3.7.7	Input and Output Capacitor	60
3.7.8	Irradiation and Temperature Sensors	61
3.7.9	16F877A Microcontroller	61
3.7.10	Voltage sensor	62
3.7.11	Current Sensor	63
3.7.12	PWM Solar Charge Controller	65
3.7.13	Battery	66
3.8	Complete PCB Diagram of Proposed PV System with MPPT Algorithm	70
3.9	Efficiency Analysis of the PV System	74

## **CHAPTER 4 - RESULT AND DISCUSSION**

4.1	Introduction	77
4.2	Analysis of Solar Energy Potential at Nibong Tebal	77
4.3	PV System Sizing	83
4.3.1	Efficiency of PV module	84
4.3.2	Peak hours of Solar Irradiation	85
4.3.3	Panel Generation Factor, PGF	86
4.3.4	Load Demand	87
4.3.5	Number of BP275F PV module needed at Nibong Tebal	88
4.3.6	Number of Matrix NP7-12 Sealed Recharged Batteries	89
4.3.7	Solar Power Inverter Rating	90
4.4	Simulation Result	90

4.4.1	DC-DC Buck Converter	90
4.4.2	PV System with P&O MPPT Technique	92
4.5	Experimental Result	96
4.5.1	Linearity of INA138 Current Sensor	96
4.5.2	DC-DC Buck Converter Prototype	98
4.5.3	DC-DC Buck Converter with P&O MPPT Controller	102
4.5.4	Stand-Alone PV System with and without MPPT Controller	103
4.6	Discussion	106
4.6.1	Analysis of Solar Energy Potential at Nibong Tebal	106
4.6.2	Simulation of PV System with P&O MPPT in Simulink	107
4.6.3	Stand-alone PV System with MPPT Control Technique	108

## **CHAPTER 5 - CONCLUSION AND FUTURE RESEARCH**

5.1	Conclusion	110
5.2	Recommendations	111

## **REFERENCES**

## **APPENDICES**

**Appendix A: Datasheet for High Efficiency BP275F PV Module**

**Appendix B: Datasheet for MOSFET IRF540N**

**Appendix C: Datasheet for INA 138 Current Shunt Monitor**

**Appendix D: Datasheet for HCPL-3140 MOSFET Driver**

## **LIST OF PUBLICATIONS**

## LIST OF TABLES

		Page
Table 3.1	Technical specifications data of BP275F 75W module	14
Table 3.2	DC-DC buck converter calculated parameters	21
Table 3.3	Battery's state of charge indication level	67
Table 4.1	A daily available sunlight for PV module	82
Table 4.2	Average of solar irradiation at Nibong Tebal in October 2012	83
Table 4.3	Typical losses in PV system	86
Table 4.4	Estimation of load demand require for single house at remote area	87
Table 4.5	Simulation data of DC-DC buck converter	91
Table 4.6	Data linearity of current sensor	97
Table 4.7	Performance of DC-DC buck converter at different value of $D$	98
Table 4.8	DC-DC buck converter for battery charging application	102
Table 4.9	Stand-alone PV system with and without MPPT technique	104

## LIST OF FIGURES

	Page	
Figure 2.1	PV cell modeled as diode circuit	12
Figure 2.2	Circuit diagram of a DC-DC buck converter	15
Figure 2.3	Waveform of voltage and current	16
Figure 2.4	Equivalent circuit when switch, $S$ in <i>ON</i> mode	17
Figure 2.5	Waveform of voltage and current when switch, $S$ in <i>ON</i> mode	17
Figure 2.6	Equivalent circuit when switch, $S$ in <i>OFF</i> mode	18
Figure 2.7	Waveform of voltage and current when switch, $S$ in <i>OFF</i> mode	19
Figure 2.8	Graph of Photovoltaic Array Battery Charging Power Transfer	22
Figure 2.9	Power - Voltage curve for a PV module	23
Figure 2.10	Flow diagram of HC	24
Figure 2.11	Power-Duty, $P$ - $D$ curve of the HC method	24
Figure 2.12	Typical Perturb and Observe MPPT algorithm	26
Figure 2.13	Divergences of HC and P&O from MPP	27
Figure 2.14	The flow diagram of the incremental conductance method	30
Figure 3.1	A block diagram of the proposed system	35
Figure 3.2	Flowchart of research methodology	36
Figure 3.3	Flowchart of sizing PV system at Nibong Tebal	38
Figure 3.4	Block diagram for $V_{ref}$ adjustment	39
Figure 3.5	Block diagram for duty cycle adjustment	40
Figure 3.6	Non-isolated synchronous DC-DC buck converter with MPPT	41
Figure 3.7	Typical operation waveforms	43
Figure 3.8	Switch, $S_2$ is turn on	44
Figure 3.9	Switch, $S_1$ is turn on	44
Figure 3.10	Flowchart of the proposed MPP tracking algorithm	45

Figure 3.11	Simulation of $I_{PV}$ in Simulink model	47
Figure 3.12	Input time varying solar irradiation, $G$ under temperature of $25^{\circ}\text{C}$	48
Figure 3.13	Input constant temperature at $25^{\circ}\text{C}$	48
Figure 3.14	Waveform of PV current, $I$ vs PV voltage, $V$	49
Figure 3.15	Waveform of PV power, $P$ vs PV voltage, $V$	49
Figure 3.16	Constant solar irradiation, $G$ of $1000\text{W}/\text{m}^2$	50
Figure 3.17	Solar temperature, $T$ under constant irradiation of $1000\text{ W}/\text{m}^2$	50
Figure 3.18	Waveform of PV current, $I$ vs PV voltage, $V$	51
Figure 3.19	Waveform of PV power, $P$ vs PV voltage, $V$	51
Figure 3.20	Detailed circuit model of PV module	52
Figure 3.21	Circuit model block of PV module	52
Figure 3.22	DC-DC buck converter circuit with DC supply	53
Figure 3.23	PV systems with MPPT control technique in Simulink	54
Figure 3.24	Switching waveforms and times	58
Figure 3.25	Voltage divider	63
Figure 3.26	Connection diagram for INA138 current sensor	64
Figure 3.27	Parameters based on battery type from Matlab-Simulink	68
Figure 3.28	Nominal current discharges characteristic	69
Figure 3.29	Current discharges vs. Time	69
Figure 3.30	Arrangement of components in double layers (PCB)	70
Figure 3.31	Practical arrangement of PV system with and without MPPT	73
Figure 4.1	A daily solar irradiation and temperature variation at Nibong Tebal	78
Figure 4.2	An average daily solar irradiation at Nibong Tebal for one week	79
Figure 4.3	An hourly solar radiation variation	79
Figure 4.4	Relation between daily solar irradiation and temperature	80
Figure 4.5	Daily PV open circuit voltage curve	81
Figure 4.6	Daily average solar irradiation versus day in Nibong Tebal	84

Figure 4.7	Simulation output waveform of DC-DC buck converter	91
Figure 4.8	Simulation circuit of PV system with P&O MPPT algorithm	92
Figure 4.9	Variation of irradiation, $G$ at 0.03s to 0.05s	93
Figure 4.10	PV module operating temperatures, $T$ at 25°C	93
Figure 4.11	Waveform of PV system with P&O MPPT for battery charging	94
Figure 4.12	Waveform of PV system with P&O MPPT for $R$	95
Figure 4.13	Input current, $I_i$ versus Sensing voltage, $v_{sense}$	97
Figure 4.14	Waveform of DC-DC buck converter at duty cycle, $D = 0.5$	99
Figure 4.15	Waveform of DC-DC buck converter at duty cycle, $D = 0.8$	99
Figure 4.16	The dead time signal for high-side and low-side MOSFET drivers	100
Figure 4.17	Efficiency of DC-DC buck converter versus Duty cycle, $D$	101
Figure 4.18	Efficiency, $\eta$ versus Output power, $P_o$	101
Figure 4.19	Performance of converter with MPPT at laboratory environment	103
Figure 4.20	Voltage of PV, $V_{PV}$ in correspond to irradiation, $G$	105
Figure 4.21	Deviation of PV output power, $P_o$ with respect to irradiation, $G$	106

## LIST OF PLATES

		Page
Plate 3.1	Four BP275F PV modules at the roof of EE School building	55
Plate 3.2	Terminal panel	56
Plate 3.3	Davis Environ-Monitor	57
Plate 3.4	Data Distribution	57
Plate 3.5	50uH inductor with air-gap	59
Plate 3.6	Fast recovery diode MUR860	60
Plate 3.7	Irradiation and Temperature sensors	61
Plate 3.8	PIC16F877A microcontroller	62
Plate 3.9	EPHC10 PWM Solar Charge Controller	65
Plate 3.10	Matrix NP7-12 sealed rechargeable battery	66
Plate 3.11	Board of DC-DC buck converter with MPPT controller	71
Plate 3.12	Experimental setup in power laboratory environment	71
Plate 3.13	An experimental setup of stand-alone system PV system	72
Plate 3.14	Data logging for stand-alone PV system	72

## LIST OF SYMBOLS

<b>Symbols</b>	<b>Description</b>
$A$	Constant with respect to temperature
$B$	Ideality factor of the junction
$C$	Capacitor
$C_B$	Battery capacity
$C_{in}$	Input capacitance
$C_{iss}$	Total input capacitance
$C_{min}$	Minimum capacitance
$D$	Duty Cycle
$D_{initial}$	Duty cycle initialization
$D_m$	Freewheeling diode
$E$	Energy
$E_g$	The band gap
$f_s$	Frequency switching
$G$	Irradiation
$I(k)$	PV module output current at $k$ sampling
$I_L$	Inductor current
$I_{mpp}$	Current at maximum power point of PV
$I_{ph}$	Photocurrent source
$I_{PV}$	PV module current
$I_s$	Reverse saturation current
$I_{sc}$	Short circuit current
$k$	Boltzmann constant
$k_T$	Temperature coefficient
$L$	Inductor
$L_{min}$	Minimum inductance

$n_p$	Number of cells in parallel
$n_s$	Number of cells in series
$P$	Power
$P_{in}$	Input power
$P(k)$	PV module output power at $k$ sampling
$P_{loss}$	Power losses
$P_{mpp}$	Power at maximum power point of PV
$P_{out}$	Output power
$R$	Resistor load
$R_{pvm}$	PV module internal resistance at maximum power
$R_s$	Series resistor
$R_{sh}$	Shunt resistor
$S$	Switch
$t$	Time
$T$	Temperature
$T_a$	Sampling time
$t_d$	Delay time
$t_f$	Fall time
$t_r$	Rise time
$V_b$	Battery voltage
$V_C$	Capacitor voltage
$V_{gs}$	Gate-source voltage
$v_i$	Input voltage correspond to input current
$V(k)$	PV module output voltage at $k$ sampling
$V_L$	Inductor voltage
$V_{mpp}$	Voltage at maximum power point of PV
$V_O$	Output voltage

$V_{oc}$	Open circuit voltage
$V_{PV}$	PV module voltage
$V_{ref}$	Reference voltage
$V_s$	Supply voltage
$v_{sense}$	Sensing voltage
$W_p$	Peak Watt
$\Delta D$	Duty cycle perturbation
$\eta$	Efficiency

## LIST OF ABBREVIATION

	<b>Description</b>
A/D	Analogue to Digital
CCM	Continuous Conduction Mode
DC	Direct Current
DCM	Discontinuous Conduction Mode
DOD	Depth of Discharge
DSP	Digital Signal Processor
EPP	Estimate and Perturb and Perturb
ESR	Equivalent Series Resistance
HC	Hill Climbing
INC	Incremental Conductance
MPO	Modify Perturb and Observe
MPP	Maximum Power Point
MPPT	Maximum Power Point Tracking
PCB	Printed Circuit Board
PGF	Panel Generation Factor
PI	Proportional and Integral
PIC	Peripheral Interface Controller
P&O	Perturb and Observe
PV	Photovoltaic
PWM	Pulse Width Modulation
SOC	State of Charge
STC	Standard Test Condition

# **PEMBANGUNAN TEKNIK ALGORITMA PTKM YANG DITAMBAH BAIK BAGI PENJANAAN KUASA FOTO-VOLTIK**

## **ABSTRAK**

Tesis ini membentangkan teknik kawalan mudah yang telah digunakan dalam pengesanan titik kuasa maximum (PTKM). Sebuah algoritma baru untuk pengecasan bateri, perlindungan pengecasan berlebihan dan teknik pengesanan kuasa maximum dalam pengusikan dan pemerhatian (P&P) telah dilaksanakan. Peningkatan teknik kawalan telah mencapai kecekapan yang optimum bagi sistem FV yang berdiri sendiri. Penggunaan P&P yang lebih baik dalam penukar AT-AT buck segerak untuk penggunaan bateri caj telah mengoptimumkan kuasa maximum tersedia untuk modul FV. Reka bentuk penukar AT-AT buck segerak telah mencapai 80% kecekapan. Didapati bahawa dengan algoritma G&L PTKM yang ditambah baik telah menunjukkan peningkatan keluaran kuasa FV sebanyak 13%, jika dibandingkan dengan sistem FV tanpa implimentasi PTKM.

# **DEVELOPMENT OF AN IMPROVED ALGORITHM OF MPPT TECHNIQUE FOR PHOTOVOLTAIC POWER GENERATION**

## **ABSTRACT**

This thesis presents a simple control technique which was used in Maximum Power Point Tracking (MPPT). A new algorithm for battery charging, overcharge protection and maximum power tracking in Perturbation and Observation (P&O) technique was implemented. The improvement of the control technique had achieved an optimal efficiency for the stand-alone PV system. The application of improved P&O in synchronous DC-DC buck converter for battery charging application had optimize the maximum available power for PV module. The synchronous DC-DC buck design achieved 80% efficiency. It is found that with an improved P&O MPPT algorithm had increased maximum PV output power by 13% when compared to a PV system without MPPT implementation.

# CHAPTER 1

## INTRODUCTION

### 1.1 Research Motivation

The demand for commercial energy is projected to continue its upward trend as both the world population and the living standard increase (Nezhad, 2009). The increase in consumption is mainly driven by the expansion of industrialization. Meeting the global demand for energy is now the key challenge to sustained industrialization (Liserre et al., 2010). The exploitation of fossil fuels during centuries and an extraction of energy from nuclear processes raise environmental issue, safety and political problems.

On the other hand, it is recognized and acknowledged that renewable and non-conventional forms of energy will play crucial role in the future as they are environmentally friendly, easy to use, clean energy and are bound to become economically more feasible with increased use (Kothari, 2000). Renewable energy term is derived from a broad range of resources, all of which are based on self-renewing energy sources such as sunlight, flowing water, wind, the earth's internal heat and biomass comprise energy crops, agricultural and industrial waste, and municipal waste (Bull, 2001).

Solar energy specifically a photovoltaic (PV) is the most exploited renewable energy sources alongside with hydroelectric and wind power. Over the years, renewable energies have gone through one of the biggest growths in percentage, being comparable to the development of coal and lignite energy but still below that of natural gas. In 2007, the world's renewable energy production share has been estimated as 19%. However, 16% are attributable to hydroelectric energy production

and hence, PV energy production is still very modest. Despite the silicon inadequacy in recent years, the PV industry is growing at more than 30% annually and the cost of PV energy will reach the break-even point very soon in many countries. As of 2009, it is evident that wind energy is becoming well established with 1% of world energy production while solar energy is going through an impressive growth. In Asia and Australia, renewable energies are growing but the share within overall energy production is very divergent from country to country. The policies of Asian and Pacific countries with 35% of energy's share will perhaps be more significant in the future energy scenario. Indeed, developing countries like China and India continuously require more energy where China's energy's share has increased 1% every year since 2000 (Liserre et al., 2010).

A PV module is fabricated from a number of cells connected together, which are further interconnected in a series-parallel configuration to form PV arrays. The modules fall into several categories including mono-crystalline, poly-crystalline and thin-film. The capital cost of photovoltaic panels has fallen from more than \$ 50/W in the early 1980s to about \$ 5/W today. Eventhough this is still higher than the price of conventional base load electricity, commercial markets are booming in developing countries for remote telecommunication, remote lighting and signs, remote home and others. Investment in renewable energy resources will in the long run balance the national energy production, guarantee energy security and encourage sustainable progress (Akuru and Okoro, 2010). PV offers many advantages for instance incurring no fuel costs, not being polluted, requiring little maintenances and others. When developing a PV generation system, reliability becomes a major issue in dealing with. PV unit sizing, types and combinations of sources, energy storage technologies,

control procedures and the system internal connections are the typical considerations of reliability (Tucker and Negnevitsky, 2011).

Efficiency is another important aspect need to consider when developing a system that is based on renewable energy resources. By improving the efficiency of the systems, it will eventually improve system's reliability. PV modules still have relatively low conversion efficiency and therefore scheming maximum power point (MPP) is crucial in a PV power generation system. The PV module has a nonlinear current-voltage and power-voltage characteristics varying with irradiance and temperature that significantly affect the module power output. At the maximum power point (MPP) of I-V and P-V characteristic curves, the PV operates at its highest efficiency. Therefore, many procedures have been developed to determine MPP. MPPT stands for maximum power point tracking is a power control technique which able to find MPP and extract the maximum power available on PV module and deliver to the load through DC-DC converter. According to the development history of techniques, MPPT can be classified in two categories which are conventional techniques and artificial intelligent techniques (Khaehintung et al., 2006). The most significant conventional techniques are Hill Climbing (HC), Perturbation and Observation (P&O), Incremental Conductance (INC), Fractional Open-Circuit Voltage and Short-Circuit Current. The most applicable artificial intelligence techniques are Fuzzy Logic and Neural Network methodologies. (Esrām and Chapman, 2007) states that the methods mentioned vary in complexity, sensor required, convergence speed, cost, implementation hardware and other aspects. Among them, P&O method has been attracted much attention due its simplicity. The design and control methods to harvest maximum power available from PV module using P&O technique will be investigated in this research.

## **1.2 Problem Statement**

Until now, a number of MPPT techniques have been developed for PV systems and from all conventional MPPT techniques, they maximize the power output from modules for a given set of conditions by searching the best working point of the power curve characteristic and then controls the current through the modules or the voltage across them. The fundamental benefit of MPPT is that it can convert extra PV module voltage into additional charging current if charging application is used. If there is lots of excess voltage, lots of extra current and several hours of charging could be saved. However, there are two existing drawbacks encountered while generating power from PV modules. The first one is that, the efficiency of PV module is very low especially under low irradiation states and the second drawback is the amount of output power generated by PV module is affected by weather conditions namely irradiation and temperature. The changing irradiance or temperature alters the shape of a hill that often leads the climbing scheme to wrong directions in which eventually affect the reliability and overall performance of the PV power generation system.

## **1.3 Research Objective**

The primary objective of this research is to develop a new maximum power point tracking (MPPT) technique for photovoltaic power generation. To achieve the main objective, the sub objectives are listed below:

1. To develop a stand-alone photovoltaic (PV) system with maximum power point tracking (MPPT) technique for power generation
2. To optimize the maximum power available on PV module by deploying an improved P&O MPPT control technique with DC-DC power converters.

#### **1.4 Research Approach**

Firstly, the potential of renewable energy in Nibong Tebal is analyzed in order to estimate the available energy that can be produced by the PV system. Davis Instruments' Health Weather-Link is employed in order to store, view and plot the weather data gathered by the station which placed near the PV module. The pattern, mean, maximum and range of the solar irradiation and temperature had been studied that would give an overview characteristic of solar energy potential in Nibong Tebal. This information can be further used for sizing a PV system in correspond to the availability of solar energy potential in Nibong Tebal. Then, the DC-DC buck converter is developed to provide robust and high performance power point tracker acting as an intermediate between supply source and load. Lastly, a MPPT algorithm control method that is capable of tracking the MPP under variable changing of environmental condition is develop. After having the design and working idea of development a maximum power point tracking (MPPT) technique for PV power generation, a simulation is carried out to verify the idea and the performance of the proposed P&O MPPT algorithm by using Matlab-Simulink software. Besides having the simulation, a hardware prototype of the proposed model is built to validate the performance in the real case scenarios.

The scope of the research work generally covers three major components. The first part of the study is sizing of PV systems in Nibong Tebal, Penang. In this part, it will focus on the investigation and evaluation of the solar energy potential in Nibong Tebal by studying the solar irradiation and temperature data from the meteorological weather station at USM, Nibong Tebal. The second components that will be studied in this research work are building the Matlab-Simulink model of PV system with MPPT technique and performing the simulation according to the PV

module reference model. The Matlab-Simulink model is used to verify the MPPT control strategy in order to maximize the generated output power from the PV power generation system based on the proposed control method. The final parts of the research work are to develop hardware system of an improved perturbation and observation (P&O) maximum power point tracking (MPPT) technique for stand-alone PV power generation in Nibong Tebal.

## **1.5 Thesis Outline**

The thesis is divided into five main chapters which are the introduction, literature review, methodology, results, discussion as well as conclusions and recommendations. The outlines of the remaining four chapters are as follows

Chapter 2 will explain in details the literature review of renewable energy, solar energy and present the MPPT control that currently exist for a PV system. It also would provide an in-depth derivation of the formula as well as the theories in every single component which include PV characteristic, DC-DC buck converter, and the MPPT control strategy. The operation of DC-DC buck converter in continuous conduction mode (CCM) will be devoted. In addition, the literature survey on the work of previous researchers will be carried out. The three most used MPPT techniques are discussed. In the end, a short summary regarding MPPT control technique will be discussed in concluding remarks section at the end of this chapter.

In Chapter 3 will elaborate in details the framework of the research, started with the study the potential of solar energy and PV sizing system in Nibong Tebal. Later, the design of digital MPPT controller is discussed and follows by scheming synchronous DC-DC buck converter. Then, an improved P&O algorithm is presented

and a computer simulation is carried out in Matlab-Simulink. The hardware implementation of stand-alone PV system with MPPT technique and the evaluation of performance for the whole system is presented at the end of the chapter.

In Chapter 4, it clarifies about the analysis of simulation and experimental results as well as a stand-alone PV system with MPPT for power generation. Data are tabulated in tables and graphs are presented in a way that the significance of certain variables can be visualized better. Figures and diagrams are presented in great detail in order to aid in understanding the whole research and its benefits.

Finally, Chapter 5 will conclude this thesis. It provides a conclusion of achieving objectives set earlier in the thesis. The concluding remark together with summarized discussion, addressing issues and limitations will be justified. The recommendation for future work will also be stated in this chapter.

## **1.6 Research Contributions**

The contributions of this research are summarized below:

1. The method of sizing a PV system with the availability of solar radiation at selected sites has been produced.
2. The step by step procedure for modeling the PV module has been presented. The detailed modeling procedure will be able to give readers a detailed insight on photovoltaic research, particularly in the area of I-V and P-V characteristics of a PV module.
3. The proposed complete system has incorporated all the sub-systems which consists of current sensor circuit, voltage regulator, MOSFET drivers, bootstrap circuit and microcontroller block on a single working board for small scale stand-alone PV system and can be used as a reference model for future research in the photovoltaic field.
4. An improved perturbation and observation (P&O) MPPT algorithm with a charging battery scheme that could optimized PV output power is proposed and verified.

## **CHAPTER 2**

### **LITERATURE REVIEW**

#### **2.1 Introduction**

This chapter provides an overview of the literature pertaining to the proposed research project specifically on currently exist MPPT control strategy for a PV system. The literature review is started with the preface on the topic of renewable energy, solar energy, principle operation of PV and DC-DC converter topology. Subsequently, scholarly materials regarding MPPT control control strategy has been read, analyze and evaluate. Last section, Section 2.8 will discuss the concluding remarks of the Chapter 2.

#### **2.2 Renewable Energy**

Renewable energy system not produces any waste or pollutants that contribute to acid rain, health problem and do not involve environmental cleanup costs or waste disposal fees. A potential global climate change caused by excess carbon dioxide and other gases in the atmosphere is the latest environmental concern for the green non-government organization. For instance, world climate change is debated seriously in (Hammons et al., 2000). A power generation system using solar, wind and geothermal sources does not contribute any carbon dioxide to the atmosphere. In fact, today renewable sources of electricity help the United States avoid about 70 million metric tons of carbon emissions per year that would have been produced had that electricity being generated by fossil fuels.

Although the energy of the sun and wind has been utilized by mankind for millennia, modern applications of renewable energy technologies have been under serious development for only about 20 years (Bull, 2001). One of the most promising markets for renewable energy exist in supplying electricity to remote areas, especially in developing countries. Solar energy and wind power are not in high density and are available on an intermittent or irregular fashion. Renewable energy is not load-following. The utilization of energy and power in the industry, living, and working places may often be in different phase compared to the period of availability of renewable energy (Peiwen, 2008).

### **2.3 Solar Energy**

Photovoltaic (PV) is the most exploited renewable energy sources along with hydroelectric and wind power (Liserre et al., 2010). Photovoltaic device uses semiconductor materials such as silicon to convert sunlight to electricity. They contain no moving parts and generate no emissions while in operation. Photovoltaic devices can be used in small cells, modules, arrays and extremely modular. Photovoltaic systems require few servicing or maintenance and has typical lifetimes of about 20 years. PV modules are rated in terms of their peak output (peak Watt or  $W_p$ ), which is the maximum power that they will produce given optimum solar input and operating conditions. The average power produced will be closer to the rated peak output in locations where there is a high level of incidence radiation during the year. The output of a PV module varies depending on the amount of incident light and other factors such as temperature and the cleanliness of the cell surfaces (Mestre and Diehl, 2005). PV generation efficiency and power quality are the fundamental issues. PV power systems are usually integrated with control algorithms that have the function of ensuring maximum power point operation.

Output power of PV module is maximized only at a certain voltage level of 17V. This point, which is named maximum power point (MPP) is affected by solar irradiation and environmental temperature, so it is required some techniques in order to track the MPP. These techniques are generally called MPPT which is stand for maximum power point tracking. MPPTs utilize a power converter in series or parallel to extract maximum available energy from PV cells or modules and deliver it to the load.

#### **2.4 Principle Operation of Photovoltaic (PV)**

Photovoltaic (PV) generation exhibits numerous merits such as cleanness, low maintenance, no noise and regarded as one of the most essential renewable energy sources. A PV cell is basically a semiconductor diode whose *p-n* junction is exposed to light (Villalva et al., 2009). As sunlight strikes a solar cell, photons with energy greater than the corresponding energy of the band-gap are absorbed, causing the emergence of pair's electron-hole from a low energy states to an unoccupied higher energy level. These carriers are separated under the influence of electric fields within the junction and hence the *p-n* junction is electrically shorted creating a current flow that is proportional to the incidence of solar irradiation and temperature.

PV cells are combined in series and parallel connection to form larger units called PV modules, which are further interconnected in a series-parallel configuration to form PV arrays (Gow and Manning, 1996). PV cells can be classified into several types like as amorphous solar cell, mono-crystalline, polycrystalline solar cell and etc.

The irradiation level and temperature are the focal factors for characteristic of solar cell. Even though the solar cell panels were made with same manufacture technology, it still shows different I-V characteristics along variation of circumstance of solar irradiation and cell temperature (Jae-Hyun et al., 2001).

Generally, the equivalent circuit of a solar cell is represented by a single-diode model (Phang et al., 1984). The single-diode model composes of four components namely a photocurrent source  $I_{ph}$ , a diode parallel to the sources, a series resistor,  $R_s$  and a shunt resistor,  $R_{sh}$  as displayed in Figure 2.1.

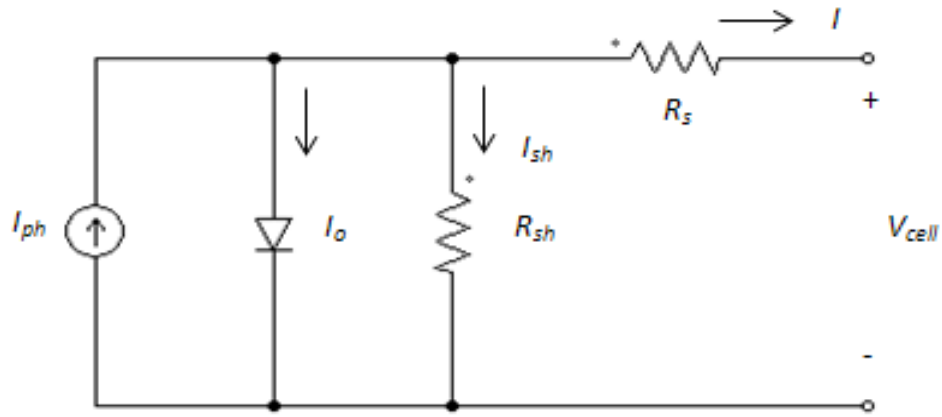


Figure 2.1: PV cell modeled as diode circuit.

The series resistance,  $R_s$  is the internal resistance of the cell and it depends on the resistance of the semiconductor. The shunt resistance,  $R_{sh}$  is due to leakage at the junction. The I-V characteristic of a PV cell is governed by the following equations:

$$I = I_{ph} - I_o - I_{sh} \quad (2.1)$$

$$I = I_{ph} - I_s \left[ \exp\left(\frac{q(V_{cell} + R_s I)}{BkT}\right) - 1 \right] - \frac{V_{cell} + R_s I}{R_{sh}} \quad (2.2)$$

where  $I_{ph}$  is the light current,  $I_s$  as reverse saturation current of the diode,  $k$  is Boltzmann constant  $1.38 \times 10^{-19}$ ,  $B$  is ideality factor of the junction,  $V_{cell}$  is voltage of PV cell and  $T$  is temperature in Kelvin. The light current,  $I_{ph}$  depends on temperature and irradiation while the reverse saturation current of the diode,  $I_s$  depends only on the temperature. Relationship between  $I_{ph}$  and  $I_s$  with irradiation,  $G$  and temperature,  $T$  is governed in Equation (2.3) and Equation (2.4) respectively.

$$I_{ph} = \frac{G}{1000} (I_{sc} + k_T (T - 298)) \quad (2.3)$$

and

$$I_s = AT^3 \exp\left(\frac{-qE_g}{BkT}\right) \quad (2.4)$$

where  $G$ ,  $I_{sc}$ ,  $k_T$ ,  $E_g$ ,  $A$  represent individually the irradiation, short-circuit current of the PV cell, the temperature coefficient, the band gap and constant with respect to temperature (Rosell and Ibáñez, 2006).

The PV cells are the basic components of all PV system. They can be connected in series to increase their operating voltage and in parallel to increase their current capacity. The total current in the PV module can be calculated as follows:

$$I = n_p I_{ph} - n_p I_s \left[ \exp\left(\frac{q(V_{cell} + R_s I) n_s}{n_s B k T} \frac{n_p}{n_p}\right) - 1 \right] - \frac{V_{cell} \frac{n_p}{n_s} + R_s I}{R_{sh}} \quad (2.5)$$

where  $n_s$  are the number of cells in series and  $n_p$  are the number of cells in parallel.

In this research, the BP275F solar module is taken as the reference model for simulation and the technical specification details are given in Table 2.1 under standard test conditions (STCs) which means an irradiation of  $1000 \text{ W/m}^2$  with an AM 1.6 spectrum at  $25^\circ\text{C}$ .

Table 2.1: Technical specification data of BP275F 75W module

<b>Description</b>	<b>Rating</b>
Rated power, $P$	75.00 W
Voltage at maximum power ( $V_{mp}$ )	17.00 V
Current at maximum power ( $I_{mp}$ )	4.45 A
Open circuit voltage ( $V_{oc}$ )	21.4 V
Short circuit current ( $I_{sc}$ )	4.75 A
Total number of cells in series ( $n_s$ )	36
Total number of cells in parallel ( $n_p$ )	1

## 2.5 DC-DC Buck Converter

A number of modules can be arranged together either in parallel or in series to form a PV array. The amount of PV output voltage depends on the arrangement of modules. A BP 275F PV module can reach out 75 W and the value of its open circuit voltage is 21.4 V. Due to the load specification and the need to provide a lower voltage with high efficiency, a regulator or converter is required in most PV applications in order to step-down the output voltage that they generate. In addition, PV modules require an intermediate power point tracker as their I-V characteristics are nonlinear (Veerachary, 2011). The proposed topology in this research is DC-DC buck converter which has the voltage output lower than the input source. The PV system is later simulated using Matlab-Simulink software.

As mentioned before, the average output voltage,  $V_o$  is less than the input voltage,  $V_s$  in a DC-DC buck converter, hence the name ‘Buck’, a very popular DC regulator for PV application. The typical circuit diagram of a DC-DC buck converter is illustrated in Figure 2.2.

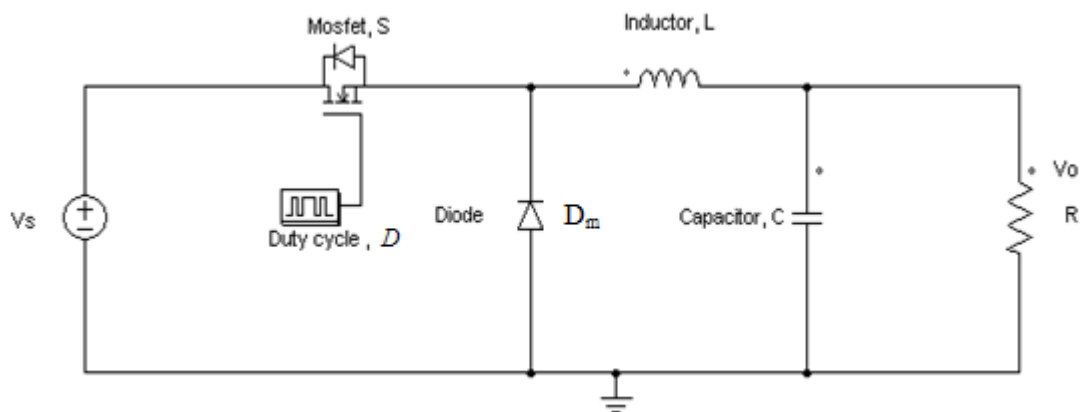


Figure 2.2: Circuit diagram of a DC-DC buck converter.

### 2.5.1 Principle of Operation

A DC-DC buck converter consists of two operating modes which are continuous conduction mode (CCM) and discontinuous conduction mode (DCM). Usually CCM technique is applied for efficient power conversion while the DCM is suitable for a lower power and stand-by application (Khader, 2011).

For the CCM, the inductor current never reaches zero during one switching cycle as illustrated in Figure 2.3. It has a smooth input current because an inductor is connected in series with the power source (Erickson, 2005).

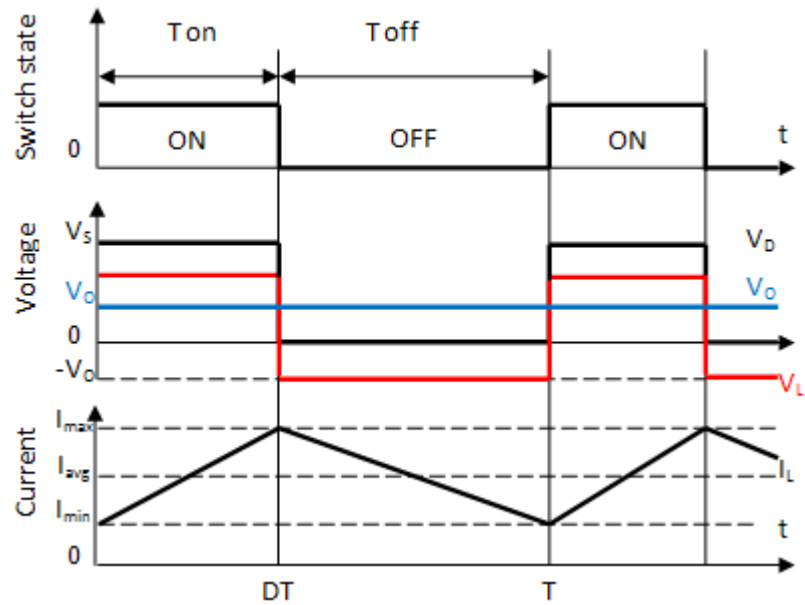


Figure 2.3: Waveform of voltage and current.

Duty cycle,  $D$  is defined as the ratio of the duration of the event to the total period of the signal and it is given by

$$D = \frac{T_{on}}{T} \quad (2.6)$$

Where  $T_{on}$  is the duration that the function is active and  $T$  is the period of the function. The value of duty cycle,  $D$  can be varied from 0 to 1. The operation of the DC-DC buck circuit can be separated into two modes wherein for mode 1, switch,  $S$  is *ON* and mode 2 wherein switch,  $S$  is *OFF*.

1) Mode 1: Switch,  $S$  is ON

The equivalent circuit for mode 1 when Switch,  $S$  is ON (during time interval,  $T_{on}$ ) and the waveforms of voltages and currents are shown in Figure 2.4 and Figure 2.5 respectively.

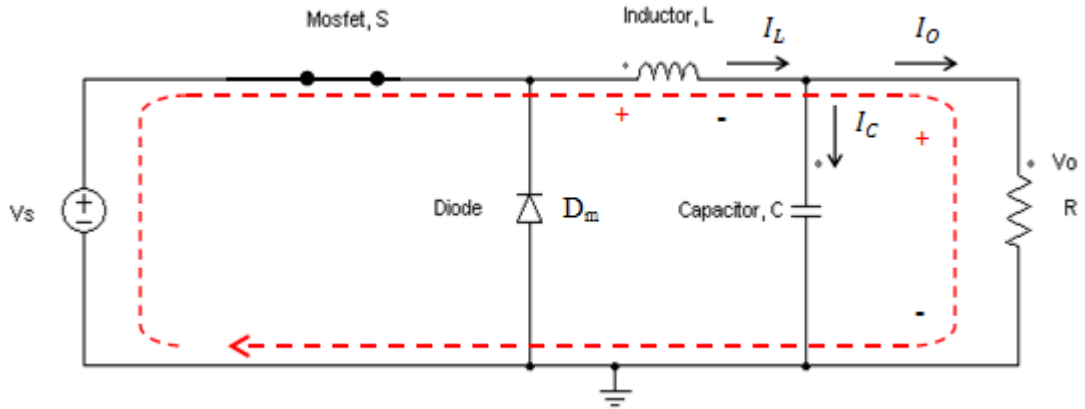


Figure 2.4: Equivalent circuit when switch,  $S$  in ON mode.

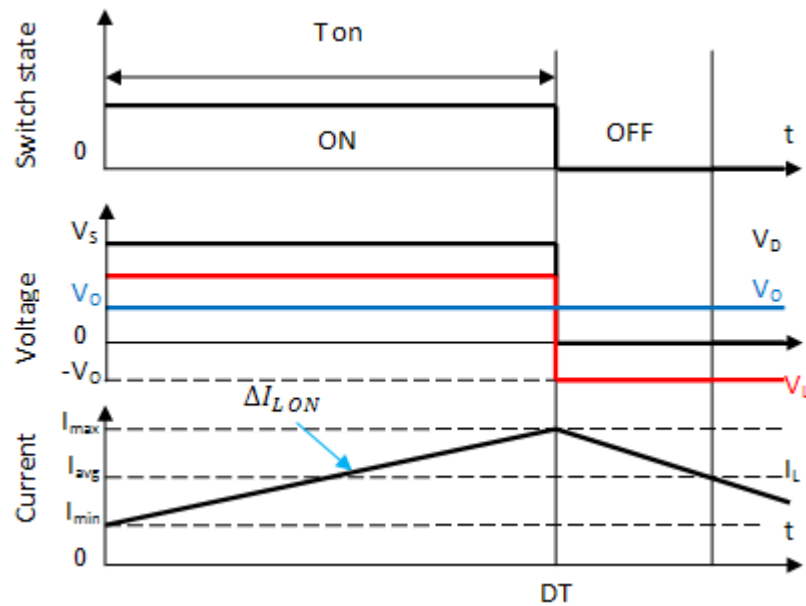


Figure 2.5: Waveform of voltage and current when switch,  $S$  in ON mode.

When switch,  $S$  is ON, the input current,  $I_L$  flows through the inductor,  $L$  filter capacitor,  $C$  and load resistor,  $R$ . By applying the Kirchhoff's voltage law, the inductor voltage,  $V_L$  is given by:

$$V_L = V_s - V_o \quad (2.7)$$

and

$$L \frac{di_{ON}}{dt} = V_s - V_o \quad (2.8)$$

Integrating  $i$  with respect to  $dt$  leads to;

$$\Delta I_{L ON} = \left( \frac{V_s - V_o}{L} \right) DT \quad (2.9)$$

where  $V_s$ ,  $V_o$ ,  $D$  and  $\Delta I_{L ON}$  are supply source, output voltage, duty cycle and value of inductor current,  $I_L$  during the  $ON$  state respectively.

2) *Mode 2: Switch S is OFF*

The equivalent circuit for mode 2 when Switch,  $S$  is *OFF* and the waveforms of voltages and currents are shown in Figure 2.6 and Figure 2.7 respectively.

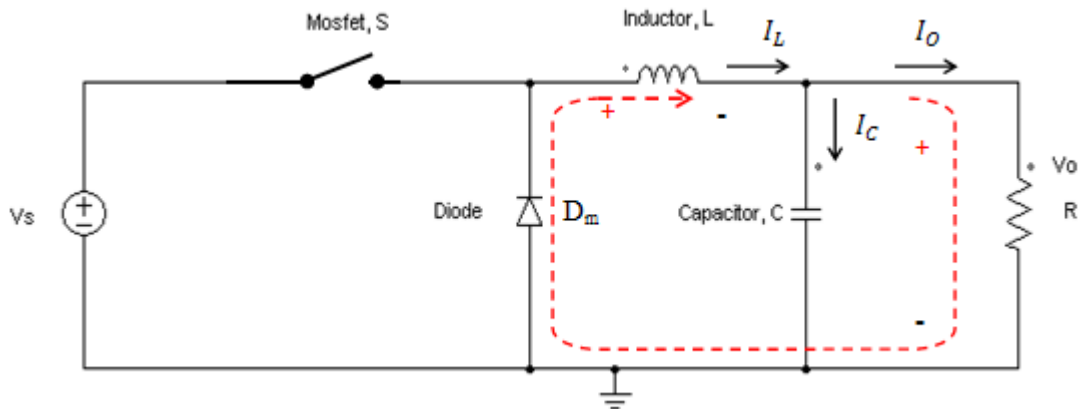


Figure 2.6: Equivalent circuit when switch,  $S$  in *OFF* mode.

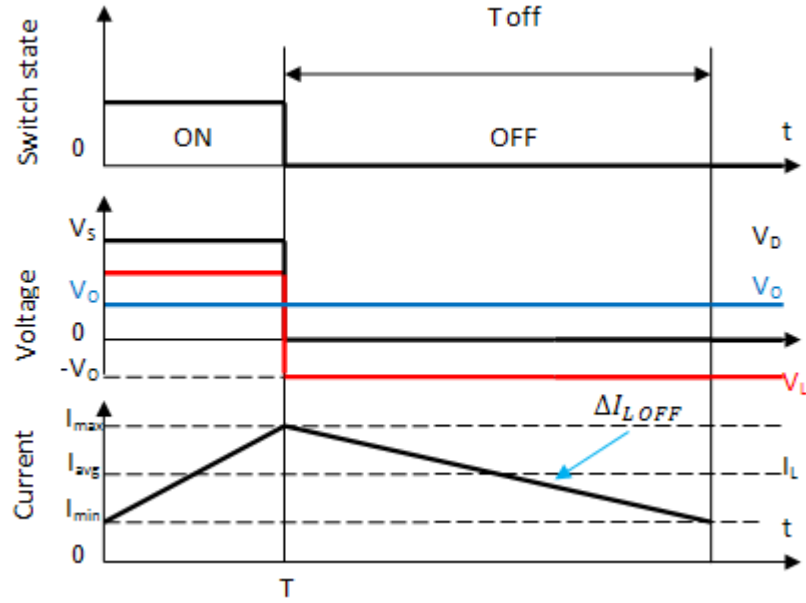


Figure 2.7: Waveform of voltage and current when switch,  $S$  in  $OFF$  mode.

When switch,  $S$  is  $OFF$  the freewheeling diode,  $D_m$  gets conducted (short circuited) due to the energy stored in the inductor and the inductor current continues to flow through  $L$ ,  $C$ ,  $R$ , and diode  $D_m$ . Therefore:

$$V_L = -V_C = -V_o \quad (2.10)$$

And

$$-V_o = L \frac{di_{OFF}}{dt} \quad (2.11)$$

Integrating  $i$  with respect to  $dt$  leads to;

$$\Delta I_{L\ OFF} = \left( \frac{-V_o}{L} \right) (1 - D)T \quad (2.12)$$

where  $V_c$  is the value of voltage across the capacitor,  $C$  and  $\Delta I_{L\ OFF}$  is the value of inductor current,  $I_L$  during  $OFF$  state.

### 3) *Steady State Operation*

During the steady state operation,

$$\Delta I_{L\ ON} + \Delta I_{L\ OFF} = 0 \quad (2.13)$$

And

$$\left(\frac{V_s - V_o}{L}\right)DT + \left(\frac{-V_o}{L}\right)(1 - D)T = 0 \quad (2.14)$$

Therefore, by solving Equation (3.14) gives the output voltage,  $V_o$  as

$$V_o = DV_s \quad ; 0 < D < 1 \quad (2.15)$$

### 4) *Continuous Inductor Current and Capacitor Voltage*

For the system to conduct current in continuous conduction mode (CCM), the minimum inductor current,  $I_L$  must be higher or equal to zero.

$$I_{min} \geq 0 \quad (2.16)$$

From (Rashid, 2004), the minimum inductance,  $L_{min}$  and capacitance,  $C_{min}$  is given by:

$$L_{min} = \frac{(1 - D)R}{2f_s} \quad (2.17)$$

And

$$C_{min} = \frac{1 - D}{16Lf_s^2} \quad (2.18)$$

where  $f_s$  is frequency switching of the MOSFET which is the reciprocal of the switching period,  $T$ . In practice, the calculated minimum value for input and output capacitor may be inadequate because output ripple voltage specifications restrain the amount of allowable output capacitor equivalent series resistance or ESR.

Attaining a sufficiently low value of ESR often requires the use of a much larger capacitor value than calculated. Taking into account that the ripple of the PV output current should be less than 2% of its mean value (Theocharis et al., 2005), and then the input capacitor value is calculated to be

$$C_{in} \geq \frac{(1 - D)(I_{om} D_{max})}{0.02 \times I_{pvm} R_{pvm} f_s} \quad (2.19)$$

where  $I_{pvm}$  is the converter input current at maximum input power,  $D_{max}$  duty cycle during maximum output power, while  $R_{pvm}$  and  $V_{inm}$  are the PV module internal resistance and the PV module output voltage at the maximum power point respectively and is defined as

$$R_{pvm} = \frac{V_{inm}}{I_{pvm}} \quad (2.20)$$

The imperative simulation parameters are listed in Table 2.2. These parameters will be used later in designing hardware of DC-DC buck converter.

Table 2.2: DC-DC buck converter calculated parameters

Components	Value
Mosfet Switch, $S$	IRF540N
Inductor, $L$	50 $\mu$ H
Diode, $D_m$	MUR 860
Output Capacitor, $C$	220 $\mu$ F
Load, $R$	4 $\Omega$
Frequency switching, $f_s$	20 kHz
Input Capacitor, $C_{in}$	220 $\mu$ F

## 2.6 Principle Operation of Maximum Power Point Tracking, MPPT

Maximum power point tracking is a power control technique that operates the PV modules in a manner that allows the modules to produce all the power they are capable of. To get a better understanding how MPPT works, let's examine a graph of PV array battery charging power transfer as illustrate in Figure 2.8 (Woodbank, 2005).

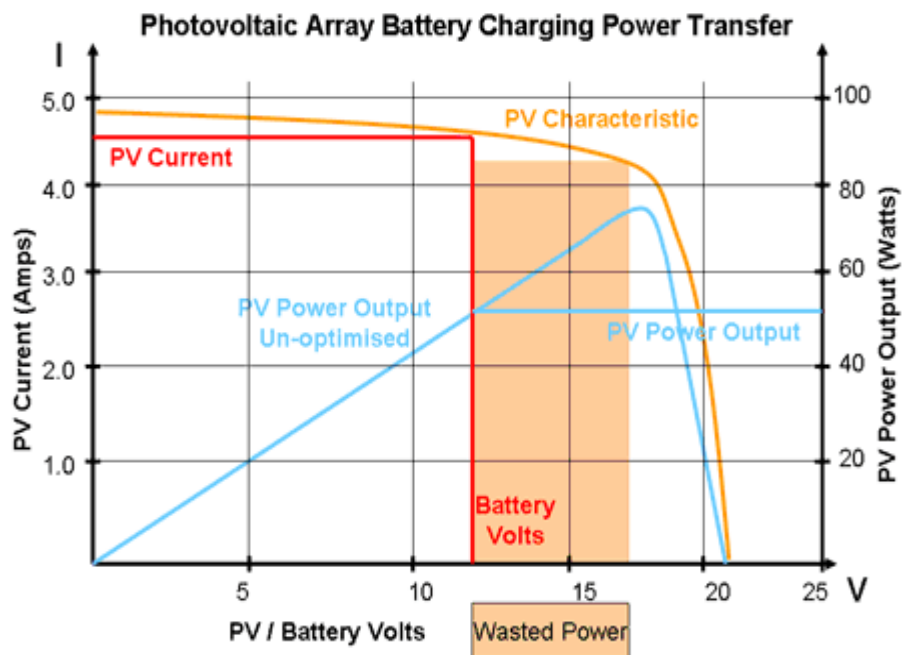


Figure 2.8: Graph of PV array battery charging power transfer.

When a conventional PV module connects directly to the battery, it will force the module to operate at battery's voltage of 12V which is not an ideal operating voltage of 17V for the available maximum power that module can generate. Therefore there is a portion of power that could not be exact from the module and it is a wasted power. The used of MPPT will vary the electrical operating point of the PV module so that the module is able to deliver the maximum available power it has.

## 2.7 Photovoltaic Control Strategy

In order to extract maximum power that PV module could harvest, researchers have come out with numbers of the control strategy. The methods vary in complexity, cost, sensor required, convergence speed, implementation hardware and other aspects. However, according to the development history of techniques, they can be classified in two categories namely conventional techniques and artificial intelligent techniques (Khaehintung et al., 2006). The most significant conventional techniques are Hill Climbing (HC), Perturbation and Observation (P&O), Incremental Conductance (INC), Fractional Open-Circuit Voltage and Short-Circuit Current. The most applicable artificial intelligence techniques are Fuzzy Logic and Neural Network methodologies. The characteristic power-voltage (P-V) curve for a PV array is shown in Figure 2.9.

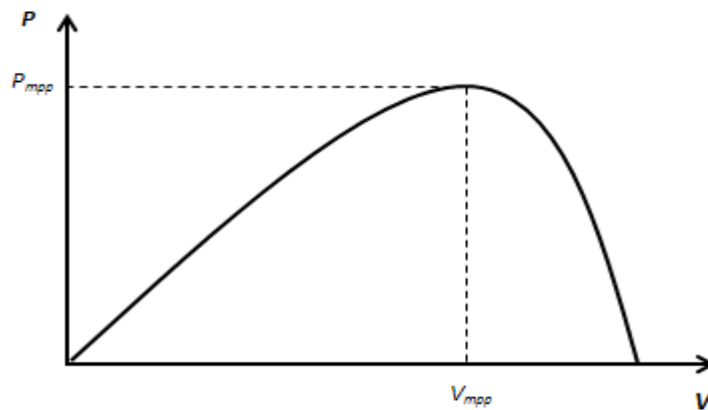


Figure 2.9: Power - Voltage curve for a PV module.

The problem raised by MPPT techniques is to automatically find the voltage  $V_{mpp}$  at which a PV module should operate to attain the maximum power output  $P_{mpp}$  under a given temperature and irradiance (Esrarn and Chapman, 2007). Several techniques as mentioned previously are discussed in details in an arbitrary order.

### 2.7.1 Hill Climbing (HC)

Hill climbing (HC) is a popular MPPT technique ever develops due to its simplicity and easy to implement. A classical HC technique as illustrate in Figure 2.10 and Figure 2.11 operated with a fixed voltage size which controls the sign of P-V curve's slope each calculation step and makes the appropriate voltage alteration.

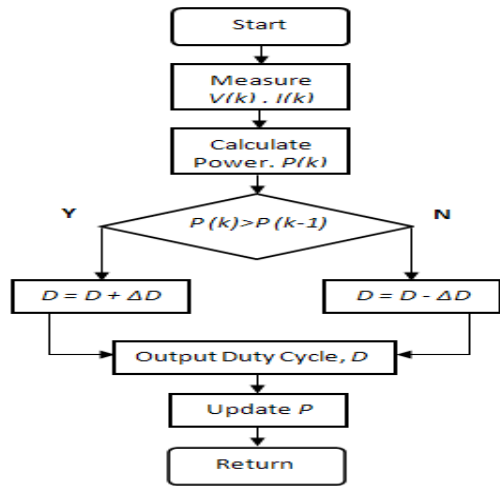


Figure 2.10: Flow diagram of HC.

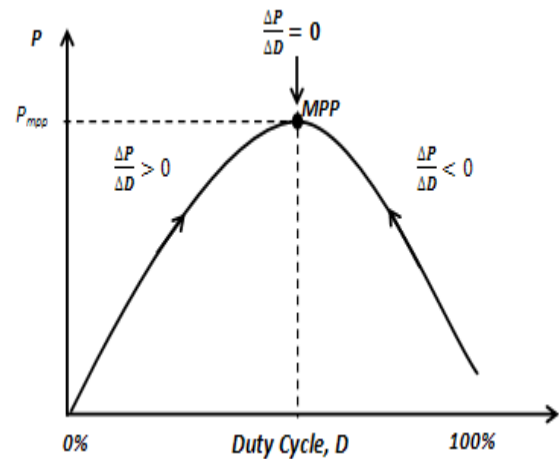


Figure 2.11: Power-Duty curve of the HC.

HC have been discussed in (Yu et al., 2002). The duty cycle,  $D$  in every sampling period is determined by the comparison of the power at the present time and previous time. If the incremental power  $\Delta P > 0$ , then the duty cycle should be increased in turn to make  $\Delta D > 0$ . Then if  $\Delta P < 0$ , the duty cycle is reduced to make  $\Delta D < 0$ .

Shortcomings of the HC method are described below. Figure 2.11 is the Power-Duty (P-D) curve diagram of PV modules when the power interface device is DC-DC buck converter. If the initial operating point of the PV system is located on the left side of the MPP, the duty cycle has to be continuously increased on the basis of the judgment procedure of the HC method in order to track the maximum power point.